applied mechanics

Article

Experimental and Theoretical Analysis of Frequency- and Temperature-Dependent Characteristics in Viscoelastic Materials Using Prony Series

Gökhan Aslan [1,*] and Nizami Aktürk [2]

[1] Graduate School of Natural and Applied Sciences, Gazi University, 06500 Ankara, Turkey
[2] Department of Mechanical Engineering, Faculty of Engineering, Gazi University, 06570 Ankara, Turkey; nakturk@gazi.edu.tr
* Correspondence: gokhan.aslan@msn.com

Abstract: This study comprehensively investigates the frequency- and temperature-dependent viscoelastic properties of two elastomer materials, focusing on the comparison between experimental results and theoretical models derived from Prony series coefficients. Dynamic Mechanical Analysis (DMA) was performed across a broad temperature range of 0–100 °C and frequency range of 0.1–100 Hz to generate storage modulus and relaxation modulus data for both materials. Relaxation tests were conducted at 25 °C to further characterize the time-dependent behavior. Time–Temperature Superposition (TTS) was applied to the resultant shift factors used to fit both Williams–Landel–Ferry (WLF) and Arrhenius equations. Additionally, sinusoidal sweep tests were carried out at 0 °C, 25 °C, 50 °C, and 80 °C, with frequencies ranging from 1 Hz to 1000 Hz, to experimentally determine the natural frequencies of the elastomers. The findings demonstrate that Prony series coefficients derived from storage modulus data offer a more accurate prediction of the viscoelastic response and natural frequencies compared to those derived from relaxation modulus data. The storage modulus data closely match the experimentally observed natural frequencies, while the relaxation modulus data exhibit larger deviations, particularly at higher temperatures. The study also reveals temperature-dependent behavior, where increasing temperature reduces the stiffness of the materials, leading to lower natural frequencies. This comprehensive analysis highlights the importance of selecting appropriate modeling techniques and data sources, particularly when predicting dynamic responses under varying temperature and frequency conditions.

Keywords: viscoelastic materials; Prony series; dynamic mechanical analysis; Time–Temperature Superposition (TTS); Williams–Landel–Ferry (WLF) equation; Arrhenius equation

Citation: Aslan, G.; Aktürk, N. Experimental and Theoretical Analysis of Frequency- and Temperature-Dependent Characteristics in Viscoelastic Materials Using Prony Series. *Appl. Mech.* **2024**, *5*, 786–803. https://doi.org/10.3390/applmech5040044

Received: 1 August 2024
Revised: 14 October 2024
Accepted: 18 October 2024
Published: 4 November 2024

1. Introduction

Viscoelastic materials, which exhibit both viscous and elastic behavior during deformation, are essential in various engineering applications, particularly for their energy dissipation and adaptability to different stress, strain, and temperature conditions. These properties make viscoelastic materials ideal for use in damping systems, automotive components, biomedical devices, and aerospace structures, where dynamic loading conditions are prevalent. A comprehensive understanding of the frequency- and temperature-dependent behaviors of these materials is crucial for optimizing their performance in real-world applications.

The viscoelastic behavior of materials is modeled using Prony series, a mathematical approach that represents the storage and relaxation modulus as a sum of exponential terms over time [1]. This model has been widely used to characterize time-dependent material responses in computational simulations and finite element analysis, enabling predictions of how materials will behave under various loading conditions [2]. Prony series models are particularly useful for simulating long-term behavior in materials subjected to dynamic loads over a broad frequency range. However, one challenge in viscoelastic modeling is

the selection of appropriate data—whether to use storage modulus or relaxation modulus data—to derive the Prony series coefficients.

Several studies have investigated the frequency- and temperature-dependent characteristics [3] of viscoelastic materials using Prony series coefficients. For instance, Silva et al. applied the Maxwell model to describe viscoelastic material behavior and demonstrated the use of shift factors to extend experimental data over a broader frequency range [4]. Other researchers have used Time–Temperature Superposition (TTS) techniques to determine shift factors for modeling materials' responses at varying temperatures [5]. Both the WLF and Arrhenius equations are widely used to fit these shift factors, providing insights into how materials soften or stiffen with temperature. However, despite these advances, a comparison of the accuracy of Prony series coefficients derived from storage modulus versus relaxation modulus data, particularly in the context of temperature- and frequency-dependent material behavior, creates a significant contribution to the field.

This study aims to address this gap by investigating which method, using storage modulus or relaxation modulus data, provides more accurate predictions of viscoelastic behavior, especially under varying temperature and frequency conditions. By comparing the Prony series coefficients derived from these two datasets, we aim to provide clarity on which approach better captures the dynamic response of viscoelastic materials.

In this research, two selected viscoelastic materials were analyzed using Dynamic Mechanical Analysis (DMA) [6] within a temperature range of 0–100 °C and a frequency range of 0.1–100 Hz. Additionally, relaxation curves at 25 °C for both materials were obtained to compare the results. TTS was applied to determine the shift factors at 5 °C intervals between 0 °C and 100 °C. These shift factors were fitted using both the WLF and Arrhenius equations. Sinusoidal sweep tests were also conducted at four temperature points (0 °C, 25 °C, 50 °C, and 80 °C) with a frequency range of 1–1000 Hz. The experimental results were then compared to theoretical models based on Prony series coefficients, derived from both storage and relaxation modulus data, to evaluate the accuracy of each method under different temperature conditions.

This study reveals that the Prony series coefficients derived from storage modulus data provide a more accurate representation of the viscoelastic materials' dynamic behavior than those derived from relaxation modulus data, particularly when considering temperature and frequency variations.

2. Materials and Method

2.1. Materials

Two different viscoelastic elastomer materials were selected for this study. These materials were chosen due to their common use in various industrial applications. The specific types and compositions of these materials are not disclosed for confidentiality reasons but are representative of typical elastomers used in engineering applications and given in Figure 1.

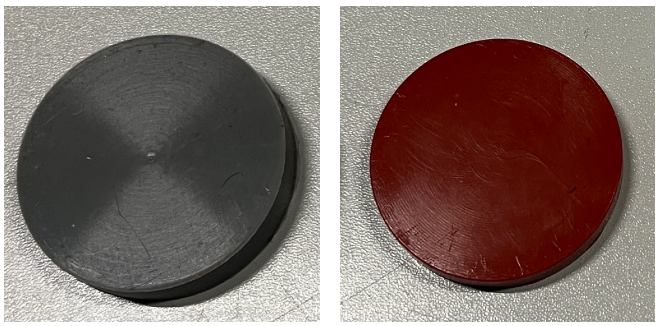

(**a**) (**b**)

Figure 1. Elastomer samples for experimental investigation. (**a**) Elastomer 1—the grey disc represents the softer elastomer. (**b**) Elastomer 2—the red disc represents the harder elastomer.

Small elastomer samples were used for the DMA analysis and Relaxation Test, while larger elastomer samples were used in the experimental setup. The physical properties (diameter, thickness, and Shore hardness) of the elastomers are presented in Table 1.

Table 1. Physical properties of elastomers used in DMA analysis, relaxation test and experimental setup.

Elastomer	Application	Diameter (mm)	Thickness (mm)	Hardness
1	DMA Analysis	11.88	6.32	20 Shore A
2	DMA Analysis	12.28	6.09	40 Shore A
1	Relaxation Test	11.21	6.22	20 Shore A
2	Relaxation Test	12.20	5.99	40 Shore A
1	Experimental Setup	50.00	9.30	20 Shore A
2	Experimental Setup	48.50	7.00	40 Shore A

2.2. Dynamic Mechanical Analysis (DMA)

Dynamic Mechanical Analysis (DMA given in Figure 2) was performed to investigate the frequency- and temperature-dependent characteristics of the selected materials. The DMA tests were conducted using a TA Instruments DMA 850 device (TA Instruments, New Castle, DE, USA). The samples were subjected to oscillatory stress in compressive mode, covering a temperature range from 0 °C to 100 °C and a frequency range from 0.1 Hz to 100 Hz. The following parameters were recorded.

- Storage modulus (G′): represents the elastic behavior of the material.
- Loss modulus (G″): represents the viscous behavior of the material.

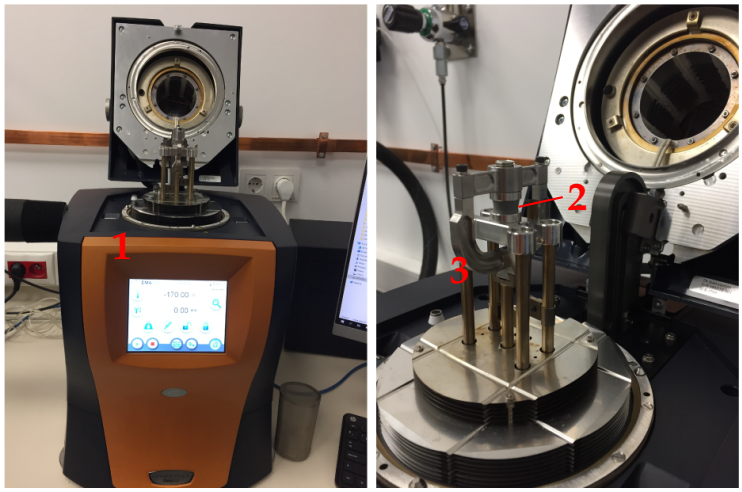

Figure 2. Dynamic Mechanical Analysis (DMA)-TA Instruments DMA 850, with labeled components: (**1**) The DMA 850 device, (**2**) Compression holding jaws, (**3**) Elastomer 1 sample located in the center of the jaws.

2.3. Shift Factor and Time–Temperature Superposition (TTS) Analysis

To extend the frequency range of the DMA data, the TTS technique was applied using the TA Instruments Trios software version 5.1.1.46572. This method allows the isothermal frequency sweep data obtained at different temperatures to be horizontally shifted along the frequency axis, resulting in a master curve that represents the material's viscoelastic behavior over a broader range of frequencies [7].

The shift factors (a_T) were determined at 5 °C intervals from 0 °C to 100 °C, employing both the WLF and the Arrhenius equations [8]:

$$\log(a_T) = -\frac{C_1(T - T_0)}{C_2 + (T - T_0)} \quad (1)$$

$$a_T = \exp\left(\frac{E_a}{R}\left(\frac{1}{T} - \frac{1}{T_0}\right)\right) \tag{2}$$

where T is the temperature, T_0 is the reference temperature, C_1 and C_2 are WLF constants, E_a is the activation energy, and R is the gas constant [9,10].

The TTS method assumes that the mechanical behavior of the material at one temperature can be related to that at another temperature by applying a horizontal shift along the logarithmic frequency axis. This shift corresponds to the shift factor (a_T), which adjusts the frequency at each temperature so that the material's response aligns with the reference temperature, creating a smooth, continuous master curve. The DMA 850 device measures the storage modulus and loss modulus across the chosen temperature and frequency ranges, and the Trios software applies the shifts to superimpose the curves.

These shift factors are essential for predicting how the material will behave over a wide range of frequencies and temperatures, which is crucial for designing materials that need to perform reliably under varying environmental conditions. In this study, both equations were fitted to the DMA data using the TA Instruments Trios software, allowing for accurate modeling of the viscoelastic properties of the tested materials [11].

2.4. Relaxation Tests

Relaxation tests were conducted at 25 °C using a TA Instruments DMA 850 device with the compression fixture to obtain the relaxation modulus curves for both materials. In these tests, the samples were subjected to a constant strain, and the decay in stress over time was measured.

The compression fixture was chosen because it ensures uniform strain distribution across the sample, which is crucial for accurate relaxation modulus measurements in viscoelastic materials.

The procedure involves applying a fixed strain to the sample while the DMA device monitored the corresponding stress over time. Initially, the material experiences an immediate elastic response, followed by a gradual decrease in stress as the material relaxes under the applied strain. This decay in stress is recorded as a function of time, generating the relaxation curve, which is a key characteristic for viscoelastic materials [12].

The relaxation modulus $E(t)$, defined as the stress divided by the applied strain over time, was calculated from the recorded data:

$$E(t) = \frac{\sigma(t)}{\epsilon_0} \tag{3}$$

where $E(t)$ is the relaxation modulus at time t, $\sigma(t)$ is the stress at time t, and ϵ_0 is the applied constant strain.

The Trios software provided by TA Instruments was used to control the test parameters and to collect the relaxation data. The obtained relaxation modulus data were then utilized to model the material's viscoelastic behavior over time using a Prony series.

2.5. Calculation of Prony Series Coefficients

Prony series coefficients were calculated using the storage modulus data and relaxation modulus data obtained at 25 °C. This process involved fitting the frequency-dependent storage modulus curve to the Prony series model using MATLAB R2020a version 9.8.0.1323502's Curve Fitting Tool (cftool) with the Levenberg–Marquardt algorithm, obtaining Prony series coefficients for the specified number of terms as described by Equation (4). Similarly, the relaxation modulus data, represented by Equation (5), were also used to verify the calculated Prony series coefficients.

The storage modulus ($G'(\omega)$) is given by [2]

$$G'(\omega) = G_e + \sum_i \frac{G_i \omega^2 \tau_i^2}{1 + \omega^2 \tau_i^2} \tag{4}$$

The relaxation modulus ($G(t)$) is given by [2]

$$G(t) = G_e + \sum_i G_i e^{-t/\tau_i} \tag{5}$$

where G_e is the equilibrium modulus, G_i are the Prony series coefficients, τ_i are the relaxation times, and ω is the angular frequency.

2.6. Shift Factors and Prony Series Coefficients

The shift factors obtained from TTS analysis are crucial in understanding the temperature-dependent behavior of viscoelastic materials. The shift factor (α_T) at a specific temperature can be used to modify the relaxation times (τ_i) in the Prony series, allowing for the prediction of material behavior across different temperatures. This is achieved by multiplying the relaxation times by the shift factor for the given temperature [5]:

$$\tau_i(T) = \tau_i \alpha_T \tag{6}$$

The modified relaxation times are then used in the state-space representation to account for temperature effects. In the A matrix (Equation (11)) of the state-space model, each term containing relaxation times is multiplied by the corresponding shift factor [4,13].

2.7. Sinusoidal Sweep Tests

Sinusoidal sweep tests were conducted at 0 °C, 25 °C, 50 °C, and 80 °C with frequencies ranging from 1 Hz to 1000 Hz. These tests were performed to investigate the dynamic behavior of the materials under various temperature conditions, and the results were compared with theoretical predictions based on Silva's Maxwell model [4].

The tests were carried out using a Climatic Chamber and the Dongling electrodynamic shaker, model ES-70LS3-550 (Dongling Technologies Co., Ltd., Suzhou, China) (Figure 3). The sweep profile used during the test is shown in Table 2, which outlines the frequency, acceleration, velocity and displacement for each test condition. The sinusoidal sweep test was controlled from the fixture that allowed the test setup to be mounted on the vibration device, while the system's frequency response was measured from the top point of the mass by an accelerometer. This configuration allowed for the precise capture of how the material responded under sinusoidal loading across different temperatures and frequencies. The response of the system to the sinusoidal sweep test was recorded under varying temperatures and frequencies to analyze the material's dynamic properties under real-world operational conditions.

Figure 3. Sinusoidal sweep test device: (1) vibration test device, (2) climatic chamber.

Table 2. Sinusoidal sweep test profile.

Frequency (Hz)	Acceleration (g)	Velocity (m/s)	Displacement (mm)
1	0.02	0.031215	4.96811
5	0.5	0.156078	4.96811
1000	0.5	0.000780388	0.000124203

2.8. Maxwell Model in State-Space Representation

A simplified diagram of a single-degree-of-freedom (SDOF) viscoelastic system based on the Maxwell model is shown in Figure 4.

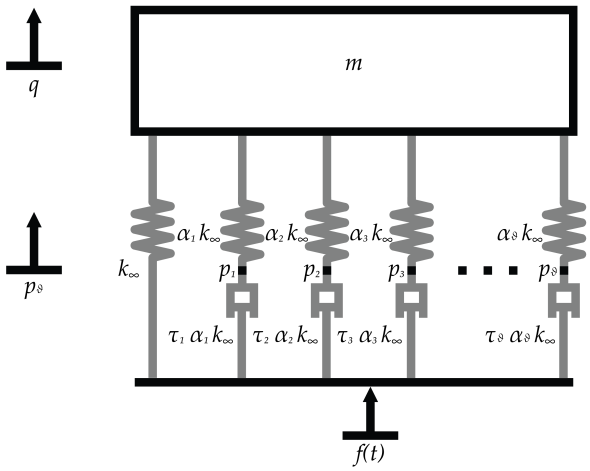

Figure 4. Maxwell model representation based on internal variable method.

The system consists of a mass (m), connected to a spring (k_∞) and several Maxwell elements in parallel. Each Maxwell element consists of a spring (k) and a dashpot (τ_i) in series, with an associated weighting factor α_n for each internal variable. The physical displacement (q) and internal degrees of freedom (p_i) are represented by the following equations [4]:

$$m\ddot{q} + k_\infty \left(1 + \sum_{n=1}^{\vartheta} \alpha_n\right) q - k_\infty \sum_{n=1}^{\vartheta} \alpha_n p_n = f(t) \tag{7}$$

$$\tau_n \dot{p}_n + p_n - q = 0, \quad n = 1, \ldots, \vartheta \tag{8}$$

Based on Silva's Maxwell model, the state-space representation is given by the following equations [4]:

$$\dot{x} = Ax + Bu(t) \tag{9}$$

$$y = Cx + Du(t) \tag{10}$$

where the A, B, C, and D matrices [4] are defined as

$$A = \begin{pmatrix} 0 & 1 & 0_{1\times\vartheta} \\ -\frac{k_\infty}{m}\left(1 + \sum_{n=1}^{\vartheta} \alpha_n\right) & 0 & \frac{k_\infty}{m}\{\alpha_n\}_{1\times\vartheta} \\ (1/\tau_n)_{\vartheta\times 1} & 0_{1\times\vartheta} & \mathrm{diag}(-1/\tau_n)_{\vartheta\times\vartheta} \end{pmatrix} \tag{11}$$

$$B = \begin{pmatrix} 0 \\ 1/m \\ 0_{\vartheta\times 1} \end{pmatrix}, \quad C = \begin{pmatrix} 1 & 0 & 0_{1\times\vartheta} \end{pmatrix}, \quad D = 0 \tag{12}$$

The Prony series coefficients and relaxation times are used to populate the A matrix.

2.9. Experimental Setup and Dynamic Frequency Response Analysis

To further investigate the dynamic behavior of the materials, larger elastomer samples were used in an experimental setup. Each sample had a constant mass placed on it, and sinusoidal sweep tests were conducted over a frequency range of 1 Hz to 1000 Hz at temperatures of 0 °C, 25 °C, 50 °C, and 80 °C. An accelerometer was placed on top of the mass to measure the changes in the system's natural frequency. The changes in the natural frequency of the system were observed using the accelerometer data, and the natural frequency points were identified and analyzed under different temperature conditions to understand the behavior of the viscoelastic materials. The experimental setup is illustrated in Figure 5.

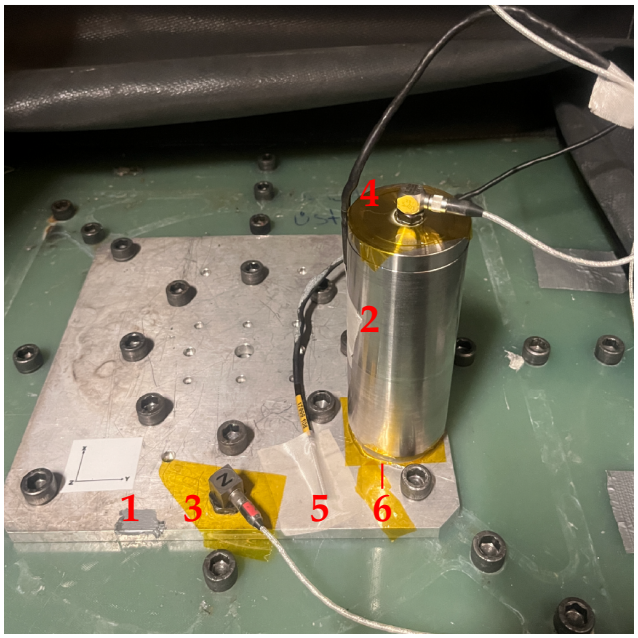

Figure 5. Experimental test setup: (1) mounting fixture, (2) mass (3.15 kg), (3) control accelerometer, (4) frequency response measurement accelerometer, (5) thermocouple, (6) elastomer.

The data obtained from the DMA were analyzed using TA Instruments Trios software for TTS analysis. Shift factor coefficients were determined to construct the shift factor curve. These coefficients, along with the fitted curves using the WLF and Arrhenius methods, were used to compare with the Prony series coefficients obtained from both the storage modulus and relaxation modulus data at 25 °C. This theoretical model was then compared to the natural frequencies obtained from the sinusoidal sweep tests conducted at different temperatures.

The comparisons focused on how well the TTS analysis coefficients, the WLF, and Arrhenius fitted shift factors and the Prony series coefficients from the storage modulus and relaxation modulus data matched the experimentally observed natural frequencies. During this analysis, both theoretical and experimental data were evaluated to understand the viscoelastic behavior of the materials under different conditions.

Additionally, the shape factor and correction factor as indicated in TA Instruments manuals [11] were applied to the raw data to update the properties of the elastomers used in the system tests. Although the manual recommended correction factor was applied, it was crucial to apply the corrections based on the natural frequency value at 25 °C in the experimental setup to ensure their accurate application.

3. Results and Discussion

3.1. The Dynamic Mechanical Analysis (DMA) and Relaxation Test Results

DMA and relaxation test results for both elastomer samples are provided in Figures 6–9. Figures 6 and 7 show the storage modulus (G') and loss modulus (G'') over a frequency range of 0.1 Hz to 100 Hz for Elastomer 1 and Elastomer 2, respectively, at various temperatures (0 °C to 100 °C in 5 °C intervals). Additionally, Figures 8 and 9 illustrate the relaxation modulus data obtained at 25 °C for both elastomer samples.

The DMA results for both elastomers in Figures 6 and 7 show a consistent increase in both the storage modulus (G') and loss modulus (G'') with increasing frequency. As expected, the viscoelastic nature of the elastomers leads to higher stiffness at higher frequencies due to reduced molecular mobility. The loss modulus (G'') also increases with temperature, indicating that the materials dissipate more energy as heat at elevated temperatures.

The relaxation test results in Figures 8 and 9 reveal the time-dependent behavior of both elastomers at 25 °C. Both materials exhibit a rapid initial decrease in the relaxation modulus, followed by a more gradual decline over time. This behavior is characteristic of viscoelastic materials, where an immediate elastic response is followed by a slower, time-dependent stress relaxation.

While Elastomer 2 shows higher initial moduli compared to Elastomer 1, both materials exhibit similar trends in the relaxation and DMA, with Elastomer 2 being stiffer overall.

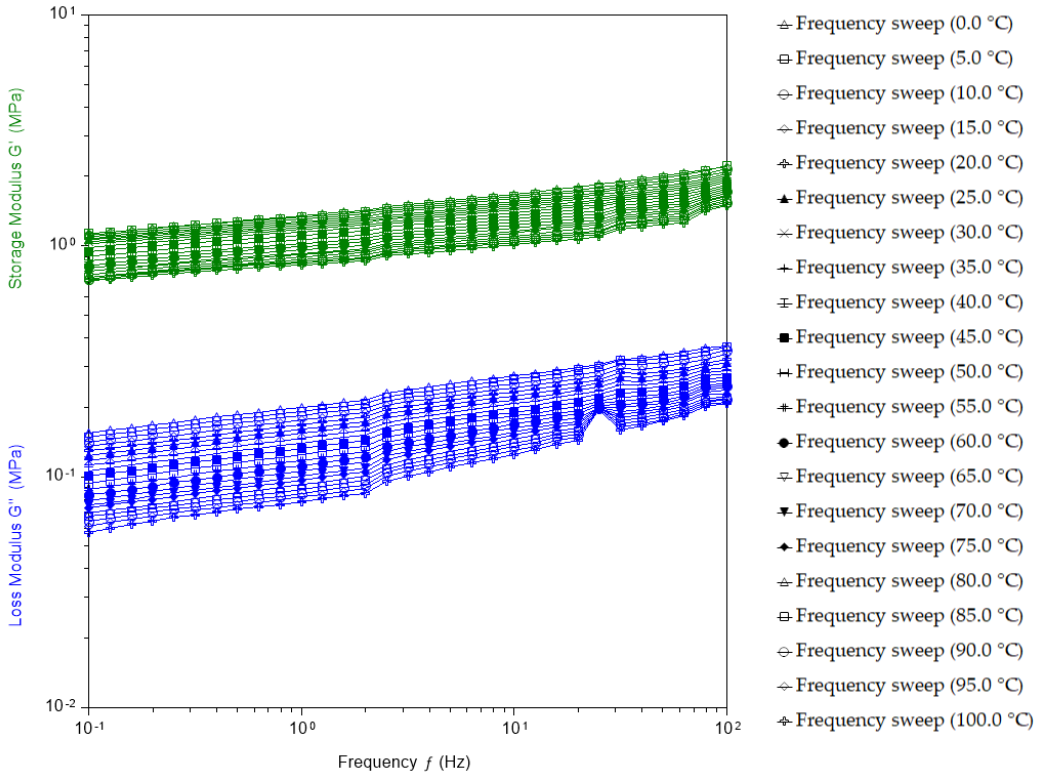

Figure 6. DMA for Elastomer 1: storage modulus (G') and loss modulus (G'') as a function of frequency and temperature.

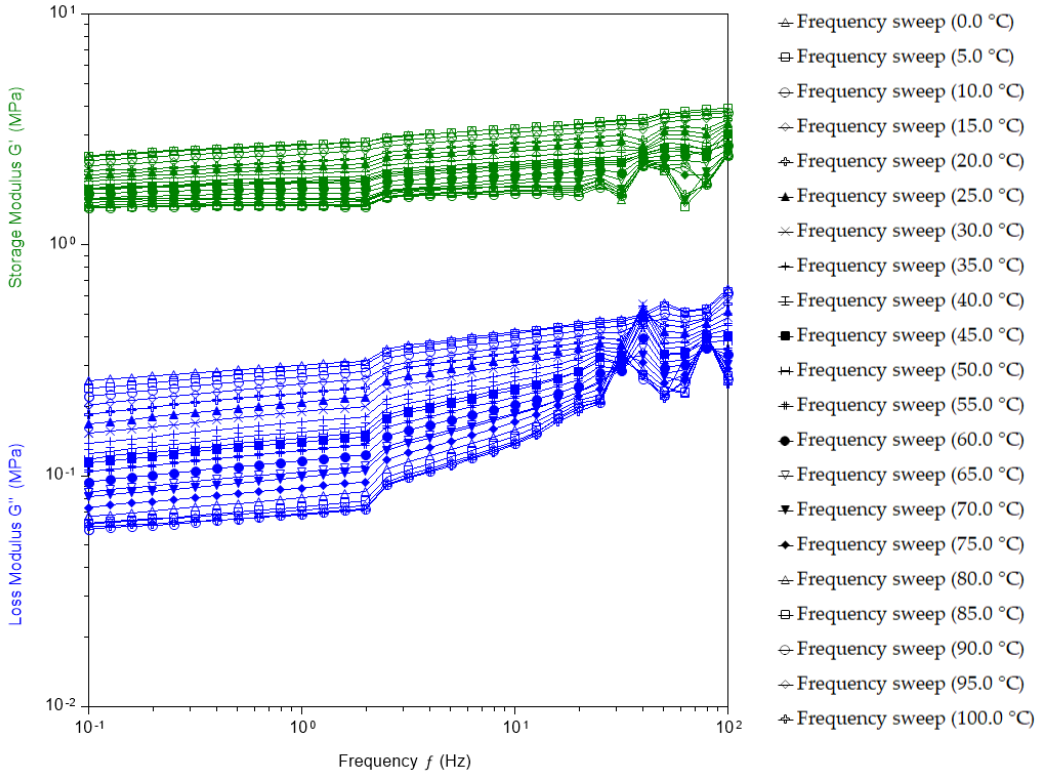

Figure 7. DMA for Elastomer 2: storage modulus (G') and loss modulus (G'') as a function of frequency and temperature.

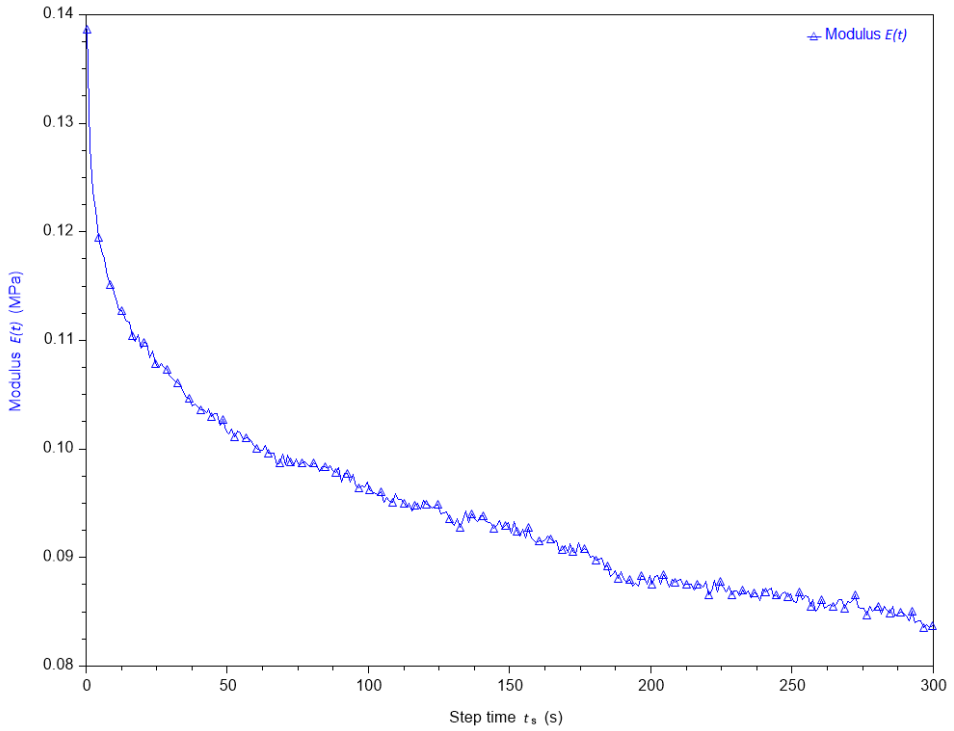

Figure 8. Relaxation modulus at 25 °C for Elastomer 1: the modulus $E(t)$ decay as a function of time.

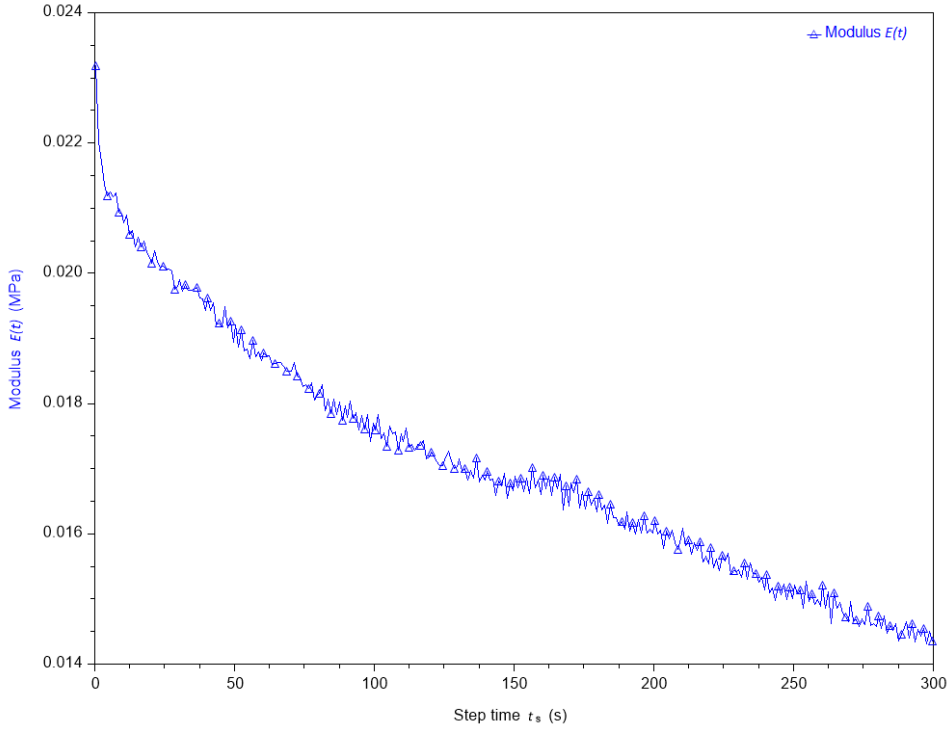

Figure 9. Relaxation modulus at 25 °C for Elastomer 2: the modulus $E(t)$ decay as a function of time.

3.2. Time–Temperature Superposition (TTS) Analysis

TTS analysis was conducted using the TA Instruments Trios software. The shift factor curves for both elastomers are presented in Figures 10 and 11. These figures include the shift factor data points and the fitted curves using both the WLF and Arrhenius equations.

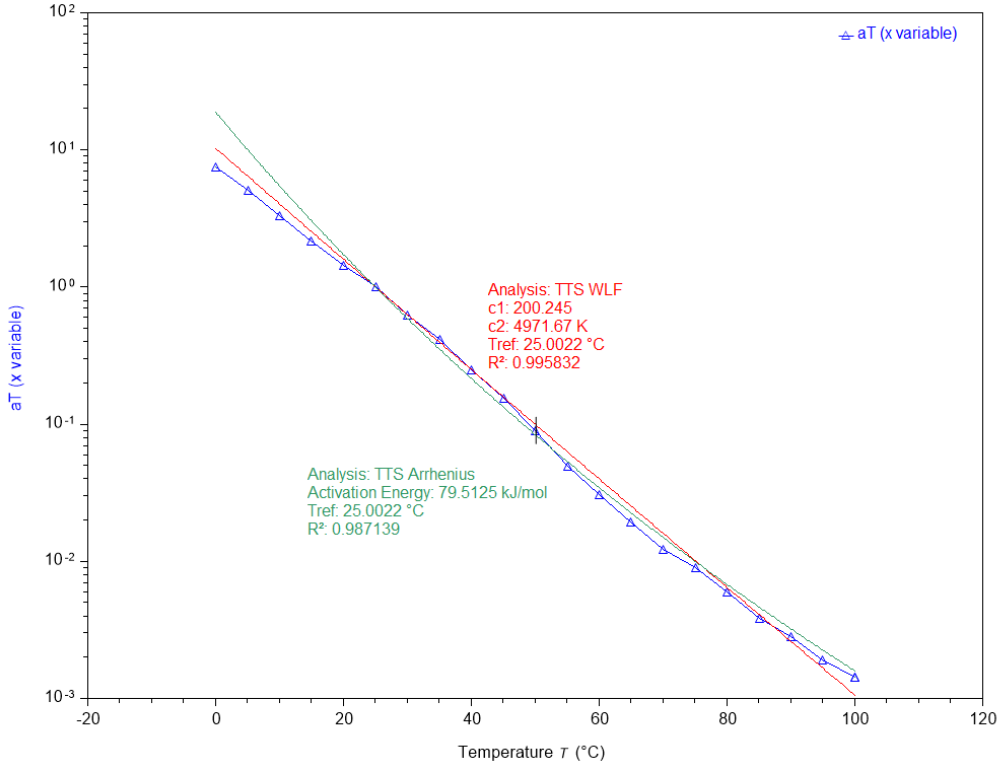

Figure 10. TTS shift factor curve for Elastomer 1. The fitted curves are based on the WLF and Arrhenius equations.

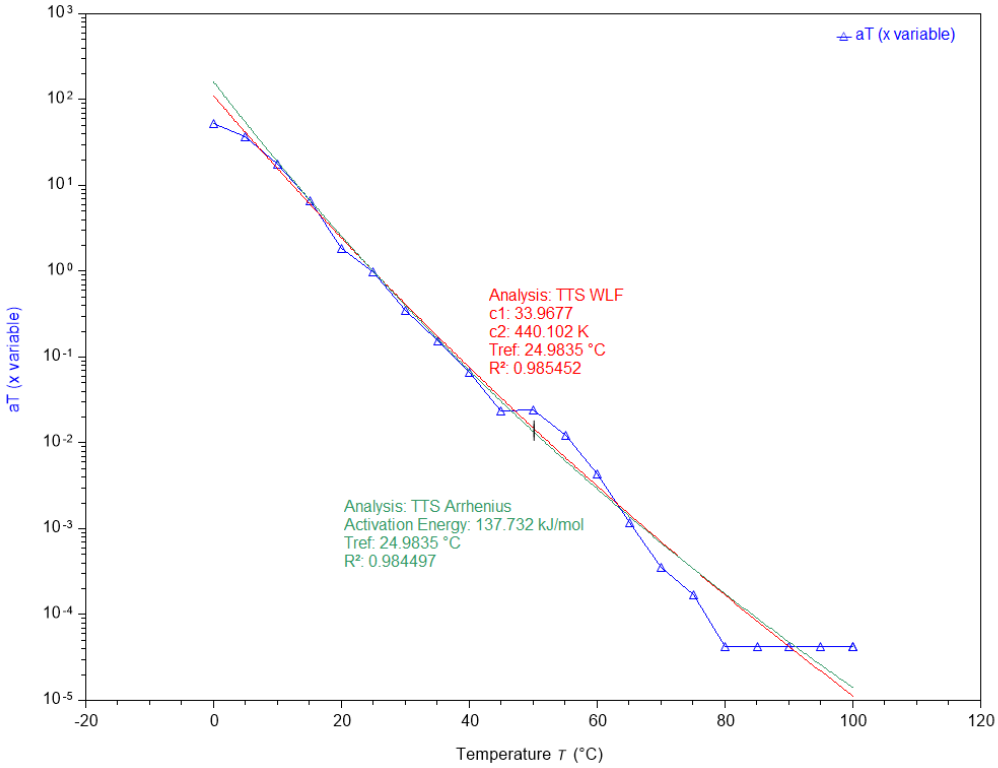

Figure 11. TTS shift factor curve for Elastomer 2. The fitted curves are based on the WLF and Arrhenius equations.

The WLF and Arrhenius parameters derived from the TTS analysis for both elastomers are presented in Table 3. These parameters provide insight into the viscoelastic behavior of the materials across different temperatures.

Table 3. WLF and Arrhenius parameters for Elastomer 1 and Elastomer 2.

Elastomer	Equation	C_1 (K)	C_2 (K)	Activation Energy (kJ/mol)
1	WLF	200.245	4971.67	-
1	Arrhenius	-	-	79.51
2	WLF	33.9677	440.102	-
2	Arrhenius	-	-	137.73

The TTS shift factor curves for both elastomers demonstrate a good fit to both the WLF and Arrhenius models as shown in Figures 10 and 11. For Elastomer 1, the WLF model provides a high correlation, with parameters $C_1 = 200.245$ and $C_2 = 4971.67$ K, and the Arrhenius equation yields an activation energy of 79.51 kJ/mol.

In comparison, Elastomer 2 exhibits slightly higher shift factor values, and the WLF parameters for this material are $C_1 = 33.9677$ and $C_2 = 440.102$ K, with an Arrhenius activation energy of 137.73 kJ/mol.

These results suggest that Elastomer 2 has a higher sensitivity to temperature changes as indicated by the higher activation energy in the Arrhenius model and the steeper slope in the WLF curve. This implies that Elastomer 2's mechanical properties are more strongly affected by temperature variations compared to Elastomer 1.

3.3. Prony Series Coefficients at 25 °C

The Prony series parameters were obtained by applying curve fitting techniques to the experimental data for both the storage modulus and relaxation modulus at 25 °C. This

approach provided the necessary coefficients to characterize the viscoelastic behavior of the elastomers. These coefficients describe the viscoelastic behavior of the elastomers, capturing both the equilibrium modulus (G_e) and time-dependent relaxation moduli (G_i) along with their associated relaxation times (τ_i). The obtained coefficients are summarized in Table 4, with all quantities provided in their respective units.

Table 4. Prony series coefficients for Elastomer 1 and Elastomer 2 at 25 °C.

Elastomer	Data Source	G_e (MPa)	G_1 (MPa)	G_2 (MPa)	G_3 (MPa)	τ_1 (s)	τ_2 (s)	τ_3 (s)
1	Relaxation	0.8607	0.3572	0.1621	0.2656	205.2	15.11	1.258
1	Storage	0.8179	0.1337	0.4707	0.2245	2.661	0.01725	0.2405
2	Relaxation	2.401	0.649	1.514	0.4538	0.01094	188.2	0.01392
2	Storage	2.607	0.7074	1.452	0.2268	0.3161	0.01133	5.288

The coefficients presented in Table 4 highlight the significant differences between Elastomer 1 and Elastomer 2, particularly in terms of the equilibrium modulus (G_e) and relaxation times (τ_i).

For Elastomer 1, the equilibrium modulus (G_e) obtained from the relaxation data is significantly lower at 0.8607 MPa, compared to Elastomer 2, which has a much higher equilibrium modulus of 2.401 MPa. This indicates that Elastomer 2 is stiffer at equilibrium, consistent with its higher Shore hardness (40) compared to Elastomer 1 (Shore hardness of 20).

In terms of the relaxation times, Elastomer 1 exhibits longer relaxation times ($\tau_1 = 205.2$ s, $\tau_2 = 15.11$ s) in the relaxation data, suggesting a slower response to stress. By contrast, Elastomer 2 has much shorter relaxation times ($\tau_1 = 0.01094$ s, $\tau_2 = 188.2$ s), which indicates that it relaxes more quickly and reaches equilibrium faster. This faster relaxation is consistent with its higher stiffness, as stiffer materials tend to relax more rapidly.

When comparing the storage modulus data, Elastomer 2 consistently shows higher values for both G_e and the Prony series coefficients (G_1, G_2, G_3) than Elastomer 1. Additionally, the relaxation times for Elastomer 2 are generally shorter, further indicating that it behaves as a stiffer and faster-relaxing material.

The large differences in the Prony parameters, particularly the significantly higher equilibrium modulus and shorter relaxation times for Elastomer 2, can be attributed to its increased stiffness and hardness. These parameters will strongly influence the dynamic performance of each elastomer as demonstrated in their Bode diagrams and natural frequency responses.

The Prony series coefficients derived for both elastomers reflect their inherent material properties, with Elastomer 2 exhibiting greater stiffness and faster relaxation times than Elastomer 1. These differences will have a substantial impact on how each material behaves under dynamic loading and temperature variation as further explored in the subsequent sections of the analysis.

3.4. Theoretical Bode Diagrams Using State-Space Analysis

The theoretical natural frequencies for the elastomers were calculated by modeling the elastomer-mass system and observing the system response in terms of amplitude and phase through a Bode diagram. The Bode diagram represents the frequency response of the system under a dynamic input, and it shows how the magnitude and phase of the output vary as a function of frequency.

The key point of interest in a Bode diagram is the resonance, where the system exhibits a peak in amplitude. This occurs because, at a certain frequency, the system enters a state of resonance, amplifying the input significantly. In the case of the elastomer-mass system, the natural frequency is defined as the frequency at which the peak amplitude occurs, indicating that the system's response to the input is at its maximum.

To determine the natural frequencies, the Prony series coefficients fitted from the storage modulus data are applied to simulate the viscoelastic behavior of the elastomers across different temperatures. By examining the Bode diagram for each temperature condition, the point of resonance can be identified, which corresponds to the natural frequency of the elastomer-mass system.

The results from the Bode diagrams show that both elastomers exhibit temperature-dependent behavior, where the natural frequency decreases with increasing temperature. This is consistent with the nature of viscoelastic materials, where higher temperatures lead to a reduction in stiffness, resulting in lower natural frequencies.

For Elastomer 1, the natural frequencies are observed around 91 Hz to 115 Hz, depending on the temperature and the type of analysis (Shift Factor Points, WLF Fit or Arrhenius Fit). As temperature increases, the system softens, which is reflected in the decrease in the natural frequency.

Similarly, for Elastomer 2, the natural frequencies range from approximately 145 Hz to 201 Hz, showing a higher stiffness compared to Elastomer 1 as evidenced by the higher natural frequencies. The temperature-dependent behavior is also visible in this case, where increasing the temperature leads to a decrease in the natural frequency values.

The WLF and Arrhenius Fits show slightly different predictions for the natural frequencies, but both are consistent with the experimental data and provide valuable insights into how each elastomer behaves under dynamic loading conditions at various temperatures. Additionally, the system responses derived from the storage modulus data provide more accurate results across the applied frequency range, particularly when considering temperature-dependent changes, compared to the system responses obtained from the relaxation modulus data. This suggests that the storage modulus data offer better predictions of system behavior across the frequency band under varying temperature conditions.

The shift factor data points and fitted curves also provide accurate predictions of how the materials' viscoelastic properties change with temperature, enabling the accurate modeling of the elastomers' dynamic response.

Overall, Bode diagrams illustrate that both the experimental and theoretical models closely align, confirming the effectiveness of the TTS analysis in capturing the temperature and frequency dependence of these materials.

Figures 12 and 13 present the calculated natural frequencies for Elastomer 1 and Elastomer 2 across the different temperature conditions, showing a clear correlation between the viscoelastic behavior and the system's dynamic response.

3.5. Experimental Test Results

The experimental data obtained from the sinusoidal sweep tests revealed the dynamic behavior of the elastomers at various temperatures. Using Simcenter Testlab version 2021.1, the results were analyzed, and the corresponding graphs were plotted to represent the data visually. The natural frequencies for both elastomers were determined from the peak response in the sinusoidal sweep tests conducted at 0 °C, 25 °C, 50 °C, and 80 °C. As shown in Table 5, the natural frequencies of both elastomers decrease as the temperature increases, which is typical for viscoelastic materials.

For Elastomer 1, the natural frequencies range from 98 Hz at 80 °C to 116 Hz at 0 °C (Figure 14). In contrast, Elastomer 2 exhibits higher natural frequencies, ranging from 157 Hz at 80 °C to 205 Hz at 0 °C (Figure 15). This difference in behavior can be attributed to the higher stiffness of Elastomer 2, as evidenced by the higher natural frequencies across the temperature range. The results confirm that as the temperature rises, both elastomers become less stiff, leading to lower natural frequencies.

The natural frequencies identified from the sinusoidal sweep tests are presented in Table 5. The results also align with the theoretical predictions made through the TTS analysis. The experimental natural frequencies are close to the theoretical values obtained from both the WLF and Arrhenius shift factor models as previously discussed.

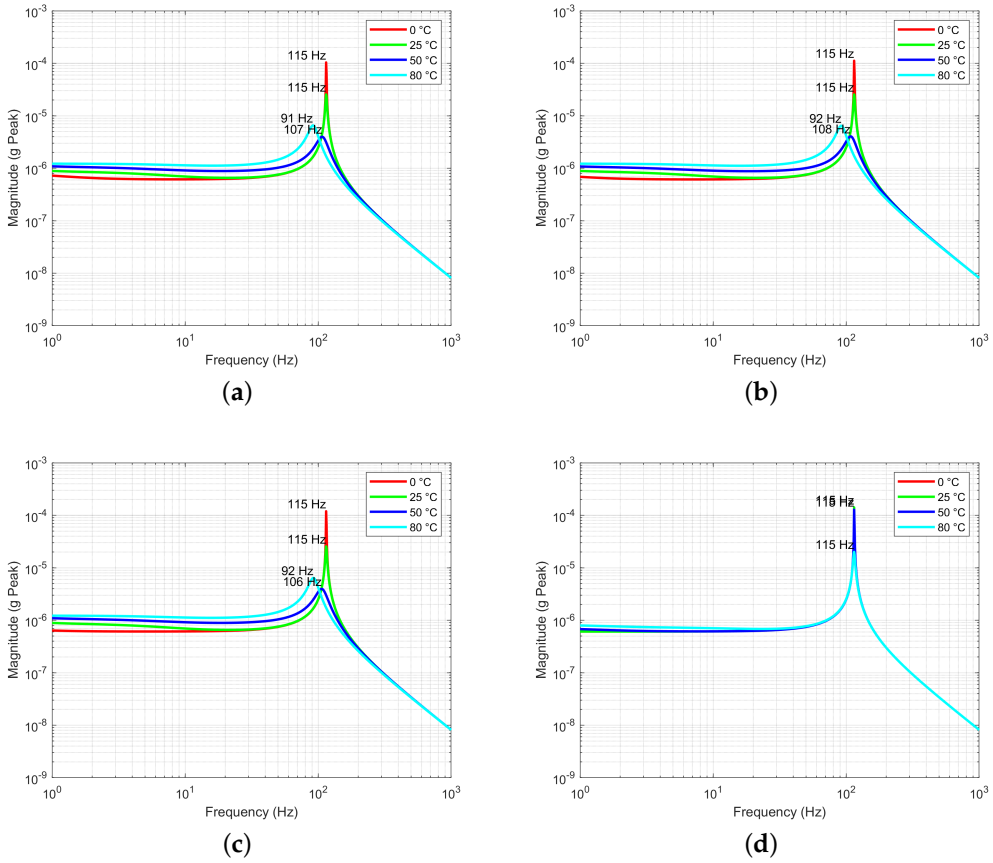

Figure 12. Theoretical natural frequency diagrams for Elastomer 1 at different temperature points. Calculation with (**a**) storage modulus data and Shift Factor Points, (**b**) storage modulus data and WLF Fit, (**c**) storage modulus data and Arrhenius Fit, (**d**) relaxation data and Shift Factor Points.

3.6. Theoretical vs. Experimental Comparison

The comparison between the theoretical and experimental natural frequencies provides valuable insights into the accuracy of the internal variable model and the effectiveness of shift factors in predicting the dynamic behavior of the elastomers. Tables 6 and 7 present the natural frequencies for Elastomer 1 and Elastomer 2, respectively, obtained from theoretical models and experimental results.

The results in Tables 6 and 7 show a strong agreement between the theoretical and experimental natural frequencies for both elastomers across all temperatures.

For Elastomer 1, the predicted natural frequencies based on the storage modulus and relaxation modulus data align closely with the experimental results, particularly at lower temperatures. At higher temperatures (80 °C), the relaxation modulus-based predictions show a slight discrepancy compared to the experimental data, likely due to the increased material softening, which is more pronounced in the experimental setup than in the theoretical models.

Similarly, for Elastomer 2, the theoretical predictions based on the storage modulus data provide accurate estimates of the natural frequencies, with only minor deviations at higher temperatures.

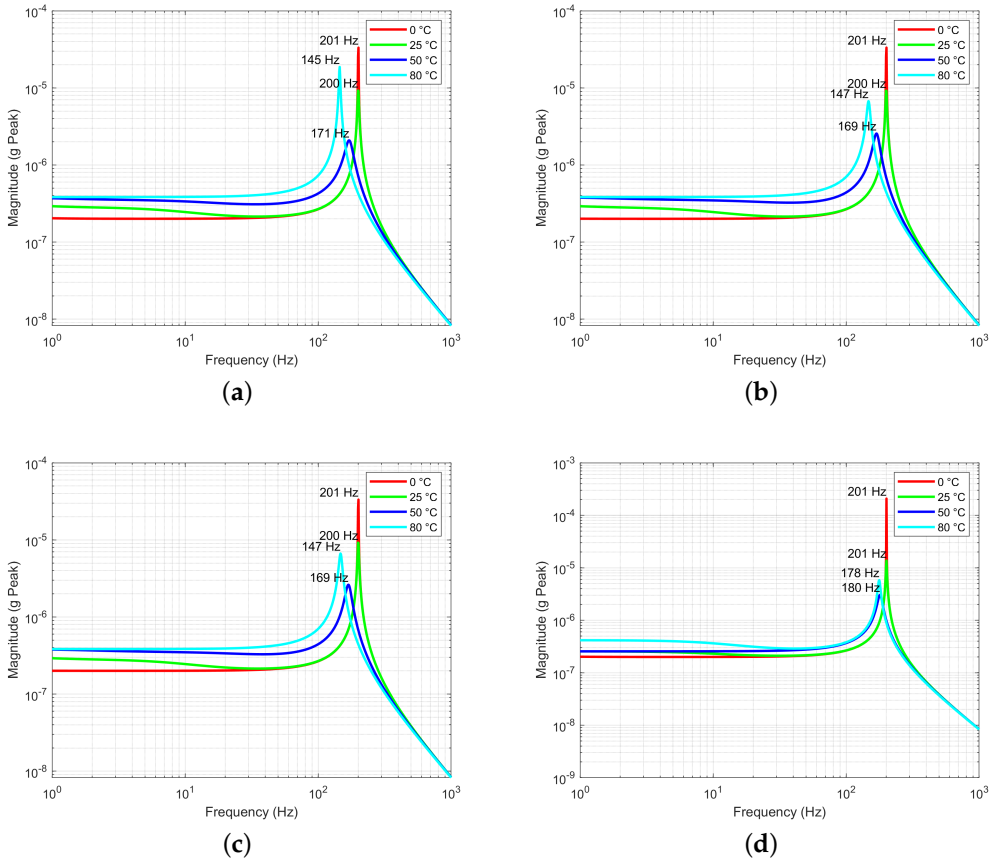

Figure 13. Theoretical natural frequency diagrams for Elastomer 2 at different temperature points. Calculation with (**a**) storage modulus data and Shift Factor Points, (**b**) storage modulus data and WLF Fit, (**c**) storage modulus data and Arrhenius Fit, (**d**) relaxation data and Shift Factor Points.

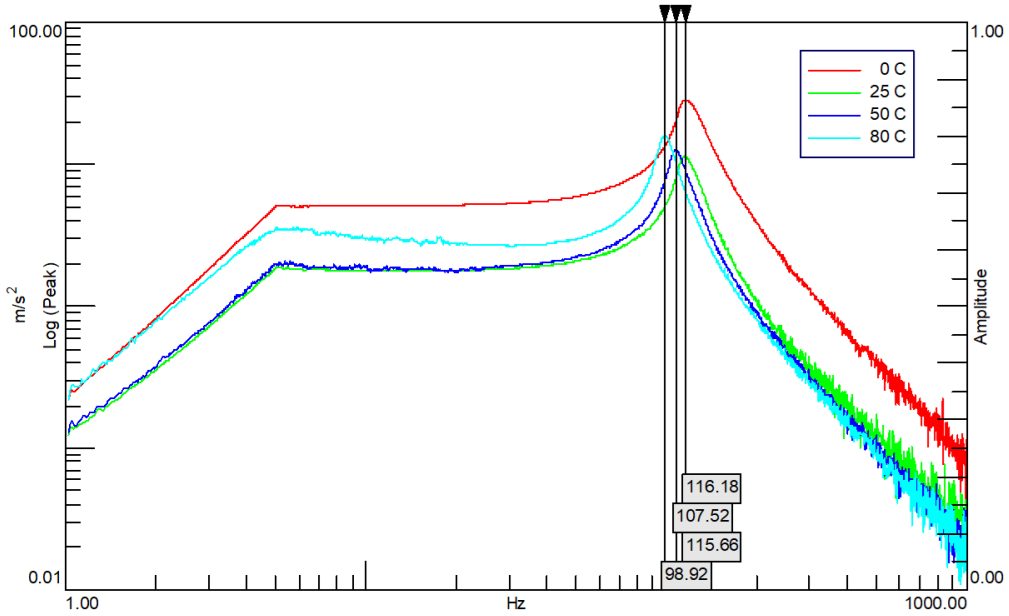

Figure 14. Experimental sinusoidal sweep test results for Elastomer 1.

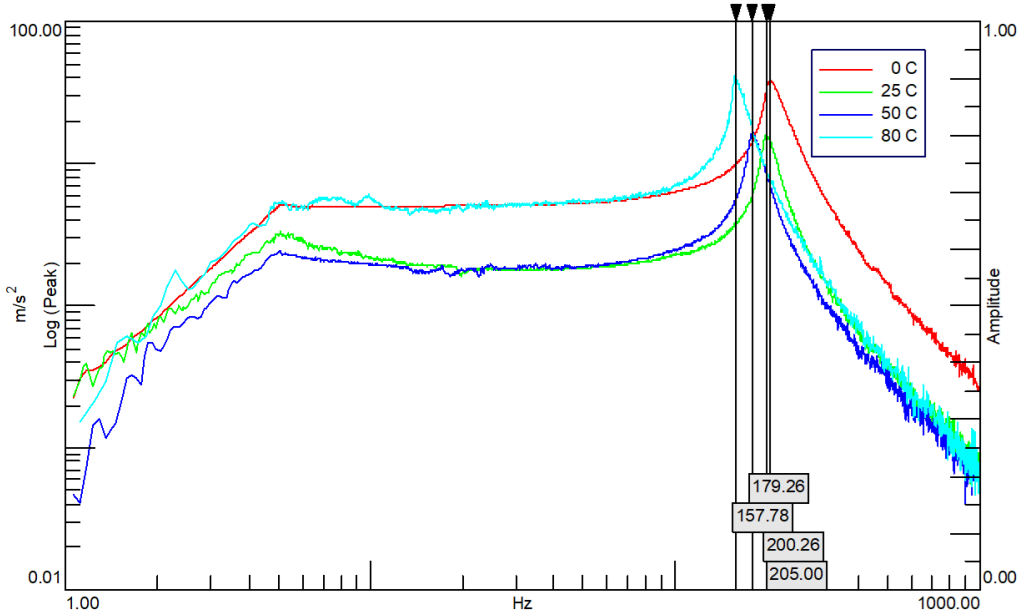

Figure 15. Experimental sinusoidal sweep test results for Elastomer 2.

Table 5. Natural frequency points for Elastomer 1 and Elastomer 2.

Temperature (°C)	Deviation (°C)	Elastomer 1 (Hz)	Elastomer 2 (Hz)
0	±2	116	205
25	±1	115	200
50	±2	107	179
80	±4	98	157

Table 6. Natural frequency points for Elastomer 1.

Temperature (°C)	Storage Modulus Shift Factor (Hz)	Storage Modulus WLF Fit (Hz)	Storage Modulus Arrhenius Fit (Hz)	Relaxation Modulus Shift Factor (Hz)	Experimental Setup (Hz)
0	115	115	115	115	116
25	115	115	115	115	115
50	107	108	106	115	107
80	91	92	92	115	98

Table 7. Natural frequency points for Elastomer 2.

Temperature (°C)	Storage Modulus Shift Factor (Hz)	Storage Modulus WLF Fit (Hz)	Storage Modulus Arrhenius Fit (Hz)	Relaxation Modulus Shift Factor (Hz)	Experimental Setup (Hz)
0	201	201	201	201	205
25	200	200	200	201	200
50	171	169	169	180	179
80	145	147	147	178	157

However, it is observed that the predictions based on the storage modulus data generally show better agreement with the experimental results compared to those based on the relaxation data.

3.7. Evaluation

During the experimental tests, it was observed that at higher temperatures, the vibration system was affected by its own cooling system. This caused the contact surface temperature of the elastomer at 80 °C to average around 76 °C, while the top surface of the elastomer averaged around 84 °C. This discrepancy explains the mismatch observed at 80 °C. However, at other temperature points, a significant convergence was observed. Among the shift factor fitting methods, no single method (WLF or Arrhenius) showed superior results over the others in this specific experiment. All methods closely approximated the experimental results. The key finding was that the Prony series coefficients obtained using the storage modulus provided a more accurate approximation than those obtained from the relaxation modulus.

4. Discussion

This study aimed to investigate the frequency- and temperature-dependent viscoelastic behaviors of two elastomer materials, referred to as Elastomer 1 and Elastomer 2, by conducting DMA and experimental tests. The storage modulus and relaxation modulus data obtained from DMA were used to calculate the Prony series coefficients, which were then applied in theoretical models to predict the natural frequencies of the elastomers. The results from these models were compared against experimental test findings.

The storage modulus data consistently provided better agreement with the experimental natural frequency results compared to the relaxation modulus data. This suggests that the storage modulus data offer a more accurate representation of the elastomers' behavior under the applied frequency range and temperature variations. One possible explanation for this observation is that the storage modulus data, which are associated with the material's elastic response, are more directly influenced by the dynamic frequency variations introduced during testing. Relaxation modulus data, on the other hand, capture the material's time-dependent stress relaxation behavior, which may not fully capture the rapid dynamics experienced in the sinusoidal sweep tests. Therefore, using storage modulus data for modeling and predicting the natural frequencies is recommended when simulating similar viscoelastic materials under dynamic loading conditions.

The theoretical predictions for the natural frequencies showed a strong correlation with the experimental results, particularly for Elastomer 1, where the predicted frequencies fit aligned closely with the experimental values. For Elastomer 2, the theoretical predictions were similarly accurate, though minor discrepancies emerged at higher temperatures. These differences may be attributed to the increased material softening observed experimentally, which may not be fully captured in the theoretical models. Despite this, the general trends in the experimental and theoretical results were consistent.

The natural frequency results also confirmed the expected temperature-dependent behavior of viscoelastic materials. As the temperature increased, the natural frequency decreased, which is characteristic of materials that become less stiff and more pliable at elevated temperatures. This behavior was observed for both elastomers, though Elastomer 2 exhibited higher natural frequencies across all temperature conditions due to its higher stiffness compared to Elastomer 1. This difference in stiffness between the two elastomers was further supported by the Prony series coefficients, where Elastomer 2 showed larger equilibrium modulus (G_e) and Prony series terms (G_i) compared to Elastomer 1. These results reinforce the importance of considering both the frequency and temperature effects when designing viscoelastic components in applications where dynamic loading and thermal exposure are expected.

In summary, the comparison of storage modulus and relaxation modulus data highlights the superior accuracy of using the storage modulus for predicting dynamic material behavior under varying frequencies and temperatures. The theoretical models based on the Prony series, combined with the shift factor fitting methods, provide a robust framework for predicting natural frequencies, with storage modulus data offering the closest match to the experimental results. These findings are essential for engineers and researchers who are

modeling the viscoelastic behavior of materials in applications such as vibration isolation, damping systems and other dynamic environments where temperature variations may affect the material performance.

Author Contributions: Conceptualization, G.A. and N.A.; methodology, G.A.; software tools usage, G.A.; validation, G.A. and N.A.; formal analysis, G.A.; investigation, G.A.; data acquisition and post-processing, G.A.; writing—original draft preparation, G.A.; writing—review and editing, G.A. and N.A.; visualization, G.A.; supervision, N.A. All authors have read and agreed to the published version of the manuscript.

Funding: This research received no external funding.

Institutional Review Board Statement: Not applicable.

Informed Consent Statement: Not applicable.

Data Availability Statement: The datasets presented in this article are not readily available because they contain commercially confidential information. Requests to access the datasets should be directed to gokhan.aslan@msn.com.

Conflicts of Interest: The authors declare no conflicts of interest.

Abbreviations

The following abbreviations are used in this manuscript:

DMA	Dynamic Mechanical Analysis
TTS	Time–Temperature Superposition
WLF	Williams–Landel–Ferry

References

1. Tschoegl, N.W. *The Phenomenological Theory of Linear Viscoelastic Behavior: An Introduction*; Springer: Berlin, Germany, 1989.
2. Tapia-Romero, M.A.; Dehonor-Gómez, M.; Lugo-Uribe, L.E. Prony series calculation for viscoelastic behavior modeling of structural adhesives from DMA data. *Ing. Investig. Tecnol.* **2020**, *21*, 1–10. [CrossRef]
3. Ward, I.M.; Sweeney, J. *An Introduction to the Mechanical Properties of Solid Polymers*; John Wiley & Sons: Chichester, UK, 2004.
4. Silva, L.A.; Austin, E.M.; Inman, D.J. The role of internal variables on the control of viscoelastic structures. In Proceedings of the IMECE2002 ASME International Mechanical Engineering Congress & Exposition, New Orleans, LA, USA, 17–22 November 2002; Volume 33991, pp. 1–10.
5. Álvarez-Vázquez, A.; Fernández-Canteli, A.; Castillo, E.; Pelayo, F.; Muñiz-Calvente, M.; Lamela, M. A Novel Approach to Describe the Time–Temperature Conversion among Relaxation Curves of Viscoelastic Materials. *Materials* **2020**, *13*, 1809. [CrossRef] [PubMed]
6. Menard, K.P. *Dynamic Mechanical Analysis: A Practical Introduction*; CRC Press: Boca Raton, FL, USA, 1999.
7. Rouleau, L.; Deü, J.; Legay, A.; Lay, F.L. Application of Kramers-Kronig relations to time-temperature superposition for viscoelastic materials. *Mech. Mater.* **2013**, *65*, 66–75. [CrossRef]
8. Yusoff, N.I.M.; Chailleux, E.; Airey, G.D. A Comparative Study of the Influence of Shift Factor Equations on Master Curve Construction. *Int. J. Pavement Res. Technol.* **2011**, *4*, 324–336.
9. Ferry, J.D. *Viscoelastic Properties of Polymers*; John Wiley & Sons: New York, NY, USA, 1980.
10. Williams, M.L.; Landel, R.F.; Ferry, J.D. The temperature dependence of relaxation mechanisms in amorphous polymers and other glass-forming liquids. *J. Am. Chem. Soc.* **1955**, *77*, 3701–3707. [CrossRef]
11. TA Instruments. Trios Software Manual. Available online: https://www.tainstruments.com/software-downloads/ (accessed on 1 August 2024).
12. Chowdhury, P.; Suhling, J.; Lall, P. Characterization of viscoelastic response of underfill materials. In Proceedings of the 2019 18th IEEE Intersociety Conference on Thermal and Thermomechanical Phenomena in Electronic Systems (ITherm), Las Vegas, NV, USA, 28 May–1 June 2019; pp. 1321–1331.
13. Christensen, R.M. *Theory of Viscoelasticity: An Introduction*; Academic Press: New York, NY, USA, 1982.